

Received February 16, 2021, accepted March 10, 2021, date of publication March 15, 2021, date of current version March 23, 2021.

Digital Object Identifier 10.1109/ACCESS.2021.3066052

Machine Learning Enabled Wi-Fi Saturation Sensing for Fair Coexistence in Unlicensed Spectrum

MERKEBU GIRMAY^{ID}, ADNAN SHAHID^{ID}, (Senior Member, IEEE), VASILIS MAGLOGIANNIS^{ID}, DRIES NAUDTS^{ID}, AND INGRID MOERMAN^{ID}, (Member, IEEE)

IDLab, Department of Information Technology (INTEC), Ghent University-imec, 9052 Ghent, Belgium

Corresponding author: Merkebu Girmay (merkebutekaw.girmay@ugent.be)

This work was supported in part by the European H2020 Programs under Grant 952189 (5G-BLUEPRINT project) and Grant 101016499 (DEDICAT6G project), and in part by the CEF Program under Grant INEA/CEF/TRAN/M2016/1364071 (CONCORDA project).

ABSTRACT In the past few years, machine learning (ML) techniques have been extensively applied to provide efficient solutions to complex wireless network problems. As such, Convolutional Neural Network (CNN) and Q-learning based ML techniques are most popular to achieve harmonized coexistence of Wi-Fi with other co-located technologies such as LTE. In the existing coexistence schemes, a co-located technology selects its transmission time based on the level of Wi-Fi traffic generated in its collision domain which is determined by either sniffing the Wi-Fi packets or using a central coordinator that can communicate with the co-located networks to exchange their status and requirements through a collaboration protocol. However, such approaches for sensing traffic status increase cost, complexity, traffic overhead, and reaction time of the coexistence schemes. As a solution to this problem, this work applies a ML-based approach that is capable to determine the saturation status of a Wi-Fi network based on real-time and over-the-air collection of medium occupation statistics about the Wi-Fi frames without the need for decoding. In particular, inter-frame spacing statistics of Wi-Fi frames are used to develop a CNN model that can determine Wi-Fi network saturation. The results demonstrate that the proposed ML-based approach can accurately classify whether a Wi-Fi network is saturated or not.

INDEX TERMS Wi-Fi saturation, traffic load estimation, coexistence, unlicensed spectrum, machine learning, convolutional neural networks.

I. INTRODUCTION

Recently, modern industry is extending the deployment of wireless networks looking into efficient networking solutions that can increase network performance. This expansion of wireless network deployments in industry along with the rapidly growing penetration of wireless network consumer devices like smartphones and tablets have led to an exponential growth of wireless traffic demand. The Internet-of-Things (IoT) that will connect an unprecedented number of intelligent devices to next-generation mobile networks also uses a significant portion of the wireless spectrum [1]. In 2020, IoT Analytics estimated that 9.5 billion devices are connected to the Internet and forecasts a growth of 28 billion devices by 2025 [2].

The associate editor coordinating the review of this manuscript and approving it for publication was Adnan Kavak^{ID}.

Similarly, the popularity of smart mobile devices and their bandwidth hungry applications result in an explosive increase of mobile traffic demands on cellular networks which has led to scarcity of licensed spectrum. On the other hand, the unlicensed band has a wide range of spectrum resources and are therefore proposed by 3GPP for opportunistic offload of mobile networks [3].

The two unlicensed bands that are widely used today are the 2.4 GHz and 5 GHz bands. The 2.4 GHz band, with only 80 MHz spectrum, is heavily used in most regions of the world. Due to the relatively favorable propagation characteristics, 2.4 GHz is already occupied by many technologies like IEEE 802.15.4, Bluetooth, and Bluetooth Low Energy technologies that do not use the 5 GHz. In contrast, the 5GHz band has a wider bandwidth i.e., up to 500MHz. Due to its wide spectral band, 5GHz band is more appealing for wireless technologies that share the same spectrum

with different coexistence techniques. For the same reasons, the future wireless networks also propose to use the 5 GHz band [4]. In 2020, the Federal Communications Commission has also adopted a new regulation that makes 1,200 MHz of spectrum in the 6 GHz band (5.925–7.125 GHz) available for an unlicensed use [5]. The next generations of Wi-Fi and other emerging technologies such as 5G NR-U are expected to coexist in this band.

Despite the enhanced capacity, the implementation of many wireless technologies in the unlicensed bands raises serious concerns about the coexistence of co-located networks operating in the same band. One of the well-established technologies that operate in the unlicensed spectrum is Wi-Fi (also known as 802.11). 802.11g/b/ax/n are the Wi-Fi standards that use the 2.4 GHz band, while the 5 GHz Wi-Fi band (802.11a/n/ac/ax) is also widely deployed across the world. Wi-Fi utilizes the carrier sense multiple access with collision avoidance (CSMA/CA) protocol to coexist with various other wireless technologies in the unlicensed spectrum [6].

Other common technology that uses the unlicensed spectrum is LTE. In legacy LTE network, a centralized scheduling mechanism is used wherein the eNodeB (eNB) decides the time and frequency at which each User Equipment (UE) in the network transmits or receives. LTE Unlicensed (LTE-U) is the first standardized technology to use the 5 GHz unlicensed band. LTE-U is standardized by LTE-U Forum and it uses the 5 GHz unlicensed band for opportunistic offloading of mobile network traffic. Another LTE standard that uses the 5 GHz unlicensed spectrum is LTE Licensed Assisted Access (LAA). LAA is the standard version of the unlicensed LTE developed by 3GPP [7]. LTE-U and LTE-LAA use different access mechanisms to coexist with other co-located technologies. LTE-U uses Carrier Sense Adaptive Transmission (CSAT) for selecting 'ON' and 'OFF' duty cycles according to Wi-Fi transmission occupancy whereas LAA uses the Listen Before Transmit (LBT) technique (similar to Wi-Fi) [8]. Private LTE technology solutions such as Multi-Fire technology are also other technologies that are mostly implemented in the unlicensed spectrum [9].

5G New Radio in the Unlicensed band (5G NR-U) is an emerging wireless technology implemented in the unlicensed spectrum. 5G NR-U has the capability to offer the necessary technology for cellular operators to integrate the unlicensed spectrum into 5G networks. In 5G NR-U, unlicensed spectrum is used for full duplex uplink and downlink transmissions. 5G NR-U supports 5G advanced features of ultra-high-speed, high bandwidth, low latency, and improved reliability of wireless communications. For this reason, massive-scale and highly-diverse future industrial networks are showing interest towards the implementation of 5G NR-U [10]. Despite the high expectations in terms of performance claimed for 5G NR-U, its coexistence with other wireless networks in the unlicensed spectrum still needs to be proven, when commercial deployments become available.

Vehicular communication is another wireless communication system that can benefit from harmonious coexistence of

multiple technologies operating in the 5.9 GHz Intelligent Transport Systems (ITS) band (more specifically between 5.85 and 5.925 GHz). ITS-G5 and Direct Short Range Communications (DSRC) are the 802.11p standards for Vehicle to Vehicle (V2V) communications in Europe and USA respectively [11]. On the other hand, the 5G Automotive Association (5GAA) has been actively developing a cellular infrastructure for vehicular communication known as Cellular Vehicle to Everything Communication (C-V2X). C-V2X has low latency and high reliability, which makes it a good candidate for enabling delay sensitive and safety critical vehicular communications [12].

No matter which unlicensed spectral band, when multiple technologies aim to use the 5 GHz unlicensed band, the shared spectrum should be used in a fair and efficient way and further respect the (regional) spectrum regulations in this band. In this study, we focus on the coexistence of Wi-Fi and other technologies in 5 GHz band, but same solutions could be applied to other bands too. While Wi-Fi technologies are designed to coexist in the unlicensed bands (by using clear channel assessment and back-off mechanisms), cellular technologies are not. For instance, LTE is used in the unlicensed band for offloading non-critical traffic by using the similar setting used by Wi-Fi for high priority traffic and this degrades the performance of Wi-Fi [13]. Many coexistence schemes have been proposed to achieve fair and efficient spectrum sharing between Wi-Fi and other co-located technologies in the unlicensed band. In these existing coexistence schemes, a co-located technology first estimates the traffic load of Wi-Fi network either by decoding the Wi-Fi packets or by using a central coordinator that can communicate with the co-located networks. However, both schemes lead to an increase in cost, complexity, traffic overhead, and latency for operating the networks. For instance, LTE-U extracts Wi-Fi transmission occupancy by decoding Wi-Fi packets and then selects the "ON" and "OFF" time of the LTE-U duty cycle [14].

The power of deep learning methods to extract important features in classification problems such as image classification and natural language processing indicate that Machine Learning (ML)-based solutions can be used to classify saturated and unsaturated Wi-Fi networks. In this article, we present an ML-based solution using Convolutional Neural Networks (CNNs) that identifies the saturation of a Wi-Fi network based on statistics of Wi-Fi frames. ns-3 simulator is used to model the saturated and unsaturated Wi-Fi networks examined in this study. A Wi-Fi network is distinguished as saturated network if its aggregated throughput has reached the maximum system throughput limit [15]. Otherwise, the Wi-Fi network is classified as unsaturated Wi-Fi network. Once the Wi-Fi network reached its saturation point, the throughput cannot increase as the offered load increases. More details on the saturated and unsaturated Wi-Fi networks can be found in Section III. The statistics used to develop our CNN models include a) histogram of Inter-frame Spacing (IFS), b) average duration of IFS and c) collision percentage

of frames. From these three statistics (features), three CNN models are developed with different combinations of the three features. The main goal of the CNN models is to distinguish between saturated and unsaturated Wi-Fi traffic. Note that later on in the paper, we will use the terms ‘statistics’ and ‘features’ interchangeably. The proposed CNN models can be implemented with the help of technology recognition module proposed in our previous work in [16] which is capable of identifying Wi-Fi traffic statistics in real-time. Hence, the proposed solution enhances the implementation of simple and real-time sensing of Wi-Fi network saturation. Once the saturation traffic status of Wi-Fi is determined based on the ML model, coexistence schemes can use it to make appropriate decisions on channel occupation. The key contributions of this work include:

- Modelling and analysis of Wi-Fi network traffic characteristics in terms of IFS histogram, average IFS duration and frame collision percentage.
- Design of three CNN models with different input features that can effectively classify saturated and unsaturated Wi-Fi traffic which enables autonomous selection of optimal configuration parameters that offer fair coexistence without the need of Wi-Fi packet decoding or any signaling overhead between Wi-Fi and other coexisting technologies.
- Performance evaluation of the three CNN models with different combination of input features in terms of accuracy, model complexity and difficulty of acquiring those features at run-time.
- Generalization performance of the three trained CNN models on unseen data captured in a grey region between saturated and unsaturated cases. Information on the grey region is given in Section V-A.
- Open source of the training and the unseen test datasets so that other researchers can use them and compare the performance and complexity of their models with our best model.

The remainder of this paper is organized as follows. Section II reviews some recent related studies on the coexistence of Wi-Fi and other technologies. Section III and Section IV illustrate the problem addressed in this article and the proposed solution respectively. The description of the system model used in this work is presented in Section V. This section explains the neural network model used to determine the saturation of a Wi-Fi traffic, whereas Section VI explains the results obtained in different traffic scenarios and provides a detailed performance evaluation of the proposed model. Finally, Section VII concludes the article and discusses plans for future work.

II. RELATED WORK

In this section, algorithms used in the coexistence of Wi-Fi and other technologies and approaches used to estimate the Wi-Fi network traffic status in the coexistence schemes are reviewed. We divide the related work into three parts:

a) coexistence in LTE and Wi-Fi, b) coexistence in 5G NR-U, and c) coexistence in C-V2X and 802.11p.

A. COEXISTENCE IN LTE AND WI-FI

Recently, extensive research has been conducted on the coexistence of Wi-Fi and other networks which are expected to operate concurrently in unlicensed spectrum bands, in particular on fair coexistence of LTE and Wi-Fi. In [17], a contention window (CW) size adaptation algorithm-based channel access scheme is proposed to achieve fair coexistence of LTE and Wi-Fi. Similarly, authors in [18], [19] propose a mechanism to adaptively adjust the back-off window size and LTE duty-cycle time fraction based on traffic status of a co-located Wi-Fi and the available licensed spectrum resource of the LTE-U while guaranteeing a fair coexistence between the technologies. Authors in [20] modelled allowable LTE transmission time selection which is determined by considering different targets of Wi-Fi service protection. In this work, the LTE transmission time is optimized for maximizing the overall normalized channel rate contributed by both LTE and Wi-Fi systems. Almeida *et al.* [21] propose a coexistence scheme that uses blank LTE subframes in order to give transmission opportunities to Wi-Fi. The scheme is evaluated via simulations and it is concluded that the number and the order of the blank subframes have an impact on the provided coexistence. Authors in [22]–[28] propose machine learning based autonomous selection of appropriate combinations of parameters that can provide fair coexistence between co-located LTE and Wi-Fi networks. However, the studies in [17]–[28] assume the LTE eNB can access the exact traffic requirements of the co-located Wi-Fi system. In practice, there is no dedicated common control channel between the two systems that can be used to exchange the traffic status. Hence, these proposed coexistence schemes require a system architecture modification on the two technologies to introduce a new channel for traffic status reporting. Alternatively, the LTE eNB can have extended Wi-Fi receiver features that decode the transmitted Wi-Fi packets. These additional system requirements make the implementation of the coexistence schemes challenging.

In [29] an energy detection based technique is proposed to reliably distinguish between one and two Wi-Fi Access Points (APs). In this work, the feasibility of the proposed energy detector based system is analyzed and experimentally verified by selecting appropriate detection thresholds using comprehensive measurements in realistic environments. Similarly, the study in [30] presents an algorithm that can distinguish between one and two Wi-Fi APs by using an auto-correlation function on the Wi-Fi preamble and setting appropriate detection thresholds to infer the number of operating Wi-Fi APs. The authors in [31] propose a ML-based approach to determine multiple Wi-Fi APs which uses the observed energy values of the APs. The studies in [29]–[31] propose less complex and straightforward approaches to determine the presence of multiple active APs as compared to decoding the entire Wi-Fi packet, which would require a full Wi-Fi

receiver at the LTE eNB. However, each active Wi-Fi AP can have different traffic loads and determining the number of active APs is not an appropriate measure to estimate the real status of co-located Wi-Fi networks. To achieve an efficient coexistence between Wi-Fi and other technologies, the co-located technologies must be able to estimate the traffic load status of the Wi-Fi network.

In [32], [33], CNN based models are used to perform identification of Wi-Fi transmissions from other co-located transmissions of other technologies. In our previous work a similar CNN model has been trained by capturing in-phase and quadrature-phase (IQ) samples of LTE and Wi-Fi transmissions [16]. The model is validated using commercial off-the-shelf LTE and Wi-Fi hardware equipment and it can identify the duration of each transmitted frame from each technology and the duration of idle slots. In this work, the idle time slots are used to compute the channel occupancy time (COT) percentage of Wi-Fi traffic which implicitly indicates the traffic demand of Wi-Fi. This COT is used to make adaptive selection of the transmission opportunity (TxOP) of a co-located LTE. In [34], [35], the CNN based traffic classification proposed in [16] is also used to implement coexistence schemes between private LTE and Wi-Fi. In an unsaturated Wi-Fi network, the COT can be a good indicator of the Wi-Fi traffic demand. However, the COT cannot be used to distinguish saturated and unsaturated Wi-Fi traffic and this makes the use of COT challenging when the Wi-Fi traffic is saturated (see Table 3 in Section III for details).

Authors in [36] propose a Q-learning based approach to estimate the traffic characteristics of Wi-Fi. The proposed approach provides a decision-making framework that employs carrier sensing at the LTE eNB to identify the idle time of the Wi-Fi. This work mainly aims to maximizing unlicensed LTE utilization of the idle spectral resources. J. Tan *et al.* [37] proposed a Deep Reinforcement Learning (DRL) based technique to estimate the traffic demand of Wi-Fi. In this work, DRL is used to enable the LAA LTE system to learn and predict the future Wi-Fi traffic demands by continuously observing the average number of total idle slots, average number of successful transmitted Wi-Fi packets, and average number of collisions, which can reflect the Wi-Fi traffic demands implicitly. This work entirely considers unsaturated Wi-Fi traffic. However, the parameters such as number of successful transmitted Wi-Fi packets which are observed in the DRL based Wi-Fi traffic estimation have different characteristics in saturated and unsaturated Wi-Fi traffic [15].

B. COEXISTENCE IN 5G NR-U

In [38]–[42] the use of unlicensed bands within a single radio access system named 5G over unlicensed spectrum is introduced. These studies emphasize on the performance of 5G in supporting stringent Internet of Things (IoT) use cases and discuss and compare the alternative strategies for spectrum management in unlicensed spectrum for 5G applications. However, a NR-U network system must adhere to any

applicable regulatory requirements for operation in unlicensed band, such as limits on transmit power, spectral density, and channel occupancy. Furthermore, the NR-U system must also achieve fair coexistence with other nodes of either the same or a different technology [10]. In [43] a system-level simulator that models the NR-U and IEEE 802.11 technologies coexistence is presented. The proposed NR-U model targets to model NR-U network in the currently available unlicensed spectrum bands while meeting its regulatory requirements. In [44], an overview of standardization efforts in coexistence of NR-U and Wi-Fi is presented. The authors also discuss the implementation challenges on the coexistence of NR-U and Wi-Fi. Furthermore, the authors suggest that the lessons learned from 5 GHz LTE and Wi-Fi coexistence should be used as a basis for the development of new standards for 6 GHz. Thus, the studies proposed in the coexistence of LTE and Wi-Fi in [22]–[28] can be extended towards the coexistence of NR-U and Wi-Fi. Hence, determining the traffic status of Wi-Fi without any need of a dedicated channel for signaling exchange can play a great role in enhancing the coexistence of NR-U and Wi-Fi.

C. COEXISTENCE IN C-V2X AND 802.11p

The debate for implementation of C-V2X or 802.11p is still ongoing. Both technologies are claiming the rights to operate in the 5.9 GHz band which is reserved for ITS operations [3]. If both technologies are deployed in the future, C-V2X will have to operate and possibly coexist with incumbent 802.11p as well as possibly with regular Wi-Fi users of other 802.11 modes. This coexistence problem, which is very similar to LTE and Wi-Fi coexistence in an unlicensed band, deserves further attention. IEEE 802.11p uses a random access MAC whereas C-V2X, based on LTE, employs a centralized MAC scheduling approach (C-V2X mode 3) or a distributed semi-persistent scheduling approach (C-V2X mode 4) [12]. Thus, studies on unlicensed LTE and Wi-Fi coexistence [17], [20]–[37] can be adopted for this coexistence problem too. On the other hand, the coexistence of DSRC, 801.11p and other 802.11 technologies have attracted some research attention [45]–[48].

D. ENHANCEMENTS

We have observed that many researchers propose different coexistence schemes to achieve fair and efficient coexistence of Wi-Fi and other technologies. In previous works many efforts have been done to estimate the load in a Wi-Fi network. These studies assume that there is a signaling protocol which is available between co-located networks to inform the networks about the current load, or they can decode Wi-Fi traffic, or they try to estimate the load in a Wi-Fi network. Very often load estimation is based on wrong assumptions (e.g. number of active APs, or COT), and, to the best of our knowledge none of previous studies take into account the saturation behavior of Wi-Fi. This paper proposes a coexistence, that (i) does not require any signaling protocol, (ii) does not require to decode Wi-Fi traffic, and (iii) is capable to

discriminate between saturated and unsaturated Wi-Fi network behavior, which will lead to much better decisions to control coexistence.

III. PROBLEM DEFINITION

The limitation of the licensed spectrum and its high associated cost has motivated the use of unlicensed bands. Thus, many wireless systems are emerging in the unlicensed spectrum. When another wireless network shares the same unlicensed band with a legacy Wi-Fi system, the most challenging issue is to prevent the co-located networks from severe performance degradation due to interference, while satisfying Quality of Service (QoS) requirements of the individual co-located networks and maintaining fair spectrum access.

The main problem with existing technologies such as LTE and C-V2X is that they were not designed to operate in shared spectrum bands with Wi-Fi. On the other hand, Wi-Fi is designed for operation in unlicensed bands and to avoid collision with other co-located wireless networks, in particular other Wi-Fi networks. Cellular technologies, like LTE and C-V2X technologies on one hand, and Wi-Fi on the other hand use different medium access protocols. The MAC mechanisms are not designed to operate together and will lead to performance degradation when operated concurrently in the same band [13].

In most of the existing spectrum sharing and coexistence techniques, previously proposed solutions assume that the coexisting wireless systems are perfectly aware of the Wi-Fi network status (e.g. Wi-Fi traffic demands or the number of active Wi-Fi users). These previously proposed solutions assume that all nodes from the co-located technologies can exchange the aforementioned information. However, it requires architectural modifications on the existing technologies to establish a dedicated signaling control channel between multiple independent systems in order to exchange their requirements. A technology that is designed to coexist with Wi-Fi could also deploy a Wi-Fi receiver to sense the traffic characteristics of co-located Wi-Fi systems. But this also leads to higher implementation complexity.

As a solution to the aforementioned challenges, this work proposes a solution that can distinguish saturated and unsaturated Wi-Fi traffic in real-time by analyzing the histogram distribution of IFS, average duration of IFS and percentage of collisions. These features can be derived by processing the statistics obtained from the technology recognition system proposed in our previous work [16]. The technology recognition solution also imposes additional capabilities of the LTE system as it can use the same receiver unit as the LTE transceiver system for capturing I/Q samples and can hence be easily integrated in future LTE radios. In this work, ns-3 simulator is used to model a 802.11a network and the features are generated from the Wi-Fi frames that access a channel modelled in the simulator. The ns-3 simulator is used as it is one of the prominent simulators to model wireless networks. Furthermore, by using the simulator we

can more easily control the traffic load to investigate saturated and unsaturated scenarios than in real-life experiments. This makes it convenient to make several experiments and collect sufficient dataset. The Wi-Fi network modelled in this work is composed of one AP and a variable number of actively transmitting stations which have different traffic loads. The stations connected to an AP are the Active Nodes (ANs) that generate traffic in the modelled Wi-Fi network. The topology of the modelled Wi-Fi network is shown in Figure 1. We consider 1 AP which is connected to N randomly distributed active nodes in a circular area with a radius of 25m range, ensuring that all ANs are in the same collision domain.

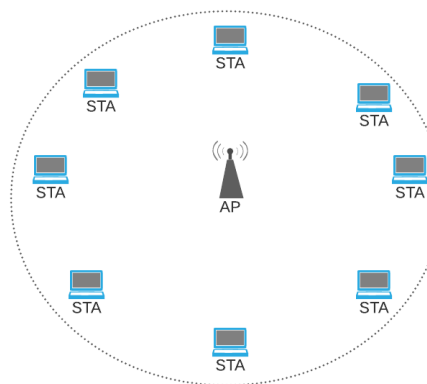


FIGURE 1. Illustration of network topology.

Table 1 shows the range of parameters used to model different scenarios of 802.11a network in the ns-3 simulator. Unless specified, the simulations discussed in this paper use the parameters presented in this table. The Short Inter-frame Spacing (SIFS) and DCF Interframe Spacing (DIFS) considered in the 802.11a network are $16\mu s$ and $34\mu s$ respectively, whereas the duration of each slot is $9\mu s$. The considered Wi-Fi network uses a constant speed propagation delay model named as *ConstantSpeedPropagationDelayModel* and a propagation loss model based on log normal distribution which is named *LogDistancePropagationLossModel* [49]. The active nodes considered in the modeled Wi-Fi network generate a User Datagram Protocol (UDP) traffic. The Packet Arrival Rate (PAR) of the UDP traffic is varied in a wide

TABLE 1. Parameters used to model different Wi-Fi traffic scenarios.

Parameter	Value
Bandwidth (MHz)	20
Carrier frequency (MHz)	5180
Packet size (bytes)	500, 1000, 1500, 2000
Traffic model	UDP
CW _{min}	15, 31, 63, 127, 255, 511, 1023
Slot duration (μs)	9
Number of ANs	1-50
SIFS (μs)	16
DIFS (μs)	34
PHY Rate (Mbps)	54
PAR (packets/sec)	5-5000

range to investigate the traffic characteristics of different load levels.

The saturation curve of the 802.11a network is shown in Figure 2 for different numbers of active nodes which use minimum contention window (CW_{min}) of 15 and maximum contention window (CW_{max}) of 1023 for a 1500 byte packet size. The graph shows how the cumulative throughput (= sum of the throughput of all active nodes in the network) varies as the packet arrival rate at the MAC queue increases. It can be observed that the maximum cumulative throughput i.e. the saturation throughput obtained depends on the number of active nodes contending for the medium.

As it can be observed in Figure 2(a), the cumulative throughput remains almost constant after a certain point even if the number of packets arriving on the MAC queue keeps increasing. This point is called the saturation point and it is represented by solid circle points in the graph. Figure 2(b) shows the number of transmitted, successful and collision frames in 10 minutes time interval for different numbers of active nodes. The results presented in this figure were obtained by setting the cumulative packet arrival rate to 2500 packets/second. The PAR indicates the number of packets arriving at the MAC queue in every second. Transmitted frames are all frames that are transmitted on the medium. Part of the transmitted frames are successful meaning that those frames can be successfully decoded and acknowledged by the receiver, while other transmissions cannot be successfully received due to collisions. Collisions occur when two or more nodes in the same collision domain transmit their frames simultaneously. It can be observed that the number of frame collisions increase with the number of active nodes competing for the shared medium. The main goal of this work is to deliver a system that can assess the characteristics of Wi-Fi traffic by analyzing the medium occupation statistics to determine whether or not the traffic load has reached this saturation point.

Table 2 shows the saturation throughput (the maximum system throughput) for 2 and 10 active nodes for different configurations of CW_{min} and the CW_{max} . The saturation throughput of each configuration is determined by increasing the PAR of the UDP traffic until it reaches the saturation point. The figure shows that the obtained saturation throughput depends on the configuration of CW_{min} and number of retransmissions(K). For fewer active nodes, the probability of frame collisions is not high even if a low CW_{min} and fewer re-transmissions are used and this leads to a high saturation throughput. However, for a large number of active nodes this configuration leads to a high frame collision probability and thereby a low saturation throughput.

For unsaturated Wi-Fi traffic, a coexisting technology can use the COT of the Wi-Fi network to take a decision on the air-time allocated to the Wi-Fi network. Table 3 shows the COT utilisation obtained in different Wi-Fi traffic scenarios. The packet sizes used in the considered scenarios are 500 byte and 1500 byte. CW_{min} was configured to 15 and CW_{max} was set 1023. The COT percentage was computed for scenarios

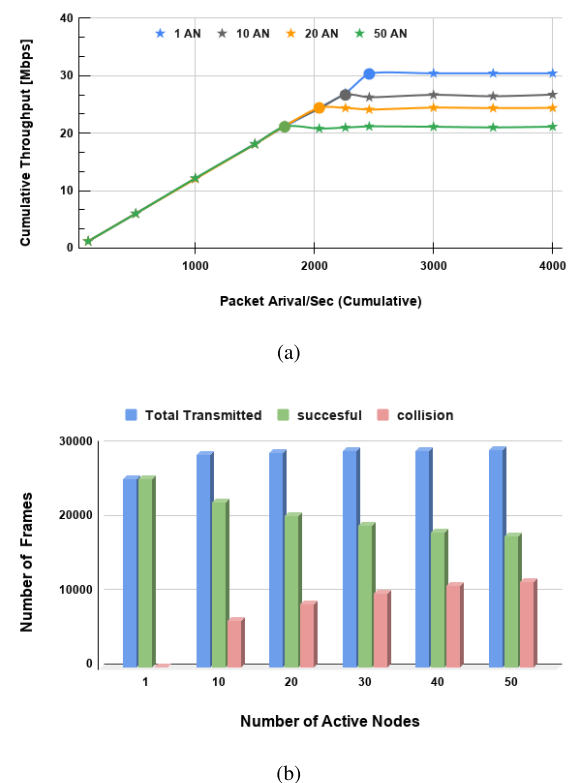


FIGURE 2. (a) Throughput saturation curves for different number of active nodes (b) Number of transmitted, successful and collided frames in during a time interval of 10 minutes with $CW_{min}=15$ and $CW_{max}=1023$ for a 1500 byte packet size.

TABLE 2. Saturation throughput of 2 and 10 active nodes for different CW_{min} and K configurations.

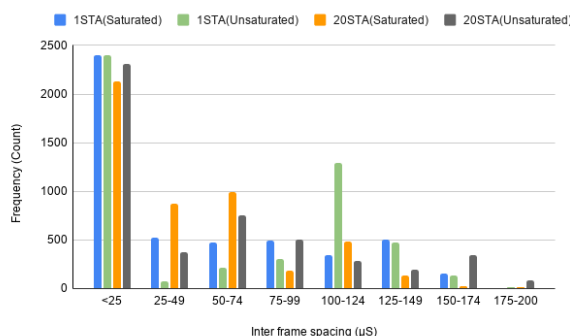
CW_{min}	Saturation Throughput (Mbps) for			
	AN=10, K=6	AN=10, K=2	AN=2, K=6	AN=2, K=2
3	22.7	15.7	29.1	26.4
7	24.8	20.1	28.9	28.8
15	26.6	23.8	29.5	29.4
31	28.4	27.2	27.7	28.1
63	29.9	29.1	23.9	24.9
127	28.5	28.5	18.2	19.2
255	25.2	24.6	12.2	13.3
511	20.7	19	8.1	9.4
1023	14.8	13.2	4.5	5.3

with 1 active node and 50 active nodes. From Table 3, we can observe that the COT percentage is not an appropriate metric to distinguish saturated and unsaturated traffic, as the same COT percentage can be achieved for saturated as well as unsaturated traffic.

In order to find out whether a Wi-Fi network is saturated or not, we also inspected the histogram of IFS distribution for saturated and unsaturated traffic scenarios as shown in Figure 3. Unfortunately, the histogram plot is not also a suitable means to discriminate between saturated and unsaturated Wi-Fi networks. This is due to the fact that IFS depends on the exponential back-off time used in frame retransmissions which on its turn depends on many parameters such as number of active nodes, PAR, CW_{min} , and CW_{max} .

TABLE 3. COT in different scenarios.

Packet Size	Number of AN	PAR/AN	COT(%)	Status
500byte	1	3000	59.8	Saturated
500byte	1	2000	50.4	Unsaturated
500byte	50	60	63.9	Saturated
500byte	50	30	47.6	Unsaturated
1500byte	1	3000	69.5	Saturated
1500byte	1	2000	53.2	Unsaturated
1500byte	50	60	73.4	Saturated
1500byte	50	30	67.8	Unsaturated

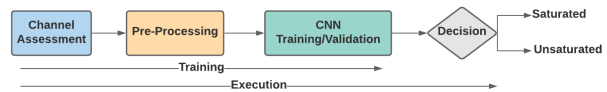
**FIGURE 3.** Histogram of Interframe Spacing.

Hence, distinguishing saturated and unsaturated Wi-Fi networks seems to be a hard problem that cannot be achieved by applying simple rules on COT statistics.

IV. PROPOSED SOLUTION

From the previous section, it becomes clear that rule-based solutions are not suitable for the identification of saturated or unsaturated Wi-Fi network. Therefore, we introduce ML techniques by developing a CNN model to identify the status of Wi-Fi traffic based on the histogram of IFS, average IFS duration, and collision percentage of the transmitted frames.

Figure 4 shows the complete architecture of the CNN based saturation sensing model (training and execution) and it comprises the following sequential steps: channel assessment, pre-processing, CNN modeling training/validation, and decision. Initially, the *channel assessment* step is done to sense the duration of each transmitted Wi-Fi frame over an operating channel. In practice, this stage can be done by capturing and processing the IQ samples of Wi-Fi traffic as described in our previous work [16]. In this work, the Wi-Fi network is modeled in the ns-3 simulator and the duration of each frame is obtained by monitoring the channel model. In the *pre-processing* step, the histogram of IFS and the average IFS duration features are extracted. The percentage of frame collisions are further obtained from the frame statistics collected in the channel assessment step. The ACK frame can be easily identified due to its short duration, typically $28\mu s$ and hence we can observe if each transmitted frame has its corresponding ACK. After generating the three features (i) histogram distribution of IFS, (ii) average IFS duration and (iii) collision percentage of the frames on the channel, the *CNN modeling training/validation*

**FIGURE 4.** Architecture of proposed solution.

step was executed in which a CNN was trained on the features to distinguish saturated from unsaturated Wi-Fi traffic. Once a CNN is trained, then in the last *decision* step, the traffic status of Wi-Fi is identified as saturated or unsaturated and the coexisting wireless network can adapt its airtime accordingly. Using the proposed model to classify saturated and unsaturated network has the following advantages:

- It helps the co-located technology to make simple coexistence decision algorithms as compared to aggregated throughput and COT based coexistence decision algorithms which depend on many parameters such as Modulation and Coding Schemes and packet size and it requires decoding and deep packet inspection of Wi-Fi frames.
- It enhances the implementation of real-time coexistence decisions as there is no delay to receive reports of Wi-Fi network traffic load status which are reported from the Wi-Fi nodes via a messaging protocol between infrastructures. This also makes it in compliance with Commercial Off-the-shelf (COTS) Wi-Fi devices as there is no need for modifying the network architecture to exchange messages for reporting Wi-Fi traffic status.
- It is compliant with all possible IEEE802.11 standards and MAC features of frame management such as frame aggregation, frame fragmentation and block acknowledgment. In the proposed scheme the statistics of IFS is used to develop a model that can determine Wi-Fi saturation. The IFS statistics is dependent on the contention window and back-off time selected based on the number of active senders contending on the medium. Therefore, the IFS histogram of saturated Wi-Fi networks has similar features even if different IEEE 802.11 standards are considered. Hence, a model trained with 802.11a network can be used with other IEEE 802.11 standards too.

V. NEURAL NETWORK MODEL FOR WI-FI SATURATION SENSING

A. DATA COLLECTION AND PROCESSING

In order to develop a CNN model that can classify saturated and unsaturated traffic, we prepared a large dataset that represents the traffic characteristics of both cases. In this dataset collection, different scenarios of saturated and unsaturated 802.11a networks were modelled using ns-3 simulator based on the parameters mentioned in Table 1. The parameters considered in preparation of the dataset were selected to cover a wide range of possible practical network configurations. The number of active stations varied from 1 to 50 (1,2,3,...,50) based on the topology shown in Figure 1.

The stations are randomly distributed within a radius of 25m. The topology and range of location of the stations were selected to consider a wide range of scenarios in the same collision domain. Packet sizes of 500, 1000, 1500, and 2000 bytes were used to represent from short to long packets. To cover a sufficient range of possible practical network configurations, minimum contention window values of 15, 31, 63, 127, 255, 511, and 1023 were considered. The PAR is tuned below and above a grey region of saturation point for saturated and unsaturated networks respectively. Once the PAR of saturation point for a specific network configuration is determined to be PAR_{sat} , the grey region is defined when the PAR lies between $PAR_{sat} - 250 \text{ packet/s}$ and $PAR_{sat} + 250 \text{ packet/s}$. UDP traffic was generated at different packet arrival rates to investigate the traffic characteristics of different load levels covering a wide range of performance variations in saturated and unsaturated traffic cases.

For each configuration and traffic load examined in this study, the simulation run-time was set to 20 minutes. Then, the starting time and duration of each frame accessing the medium is monitored to generate the IFS distribution and collision percentage. This channel monitoring is done based on frames transmitted after the first minute, as the IEEE802.11 association process takes place in the start up of the connection between the AP and the stations. Each element ε in a row of the dataset is obtained by monitoring IFS and percentage of collision and is composed of $\{x_1, x_2, \dots, x_{26}, y_1, y_2, \dots, y_{26}, \sigma, \rho, l\}$. The values $\{x_1, x_2, \dots, x_{26}, y_1, y_2, \dots, y_{26}\}$ represent the histogram of the IFS values for the M frames that accessed the medium in 1 second duration. x_{26} represents the maximum IFS duration (in ms) in the considered M frames whereas x_1 is $x_{26}/26$. The remaining x_i values are buckets at uniform spacing between x_1 and x_{26} . For $i > 1$, the values of y_i represent the IFS histogram count (in percentage) for a corresponding bucket interval between x_{i-1} and x_i . In the case of y_1 , the bucket interval is between 0 and x_1 . The σ and ρ in the sequence of the dataset element represent the average IFS duration (in ms) and percentage of frame collisions respectively. The average IFS duration is computed by averaging the IFS between each frame in the dataset element ε over the total number of frames. Similarly, the collision percentage is computed by counting the frames that are not acknowledged (if no corresponding ACK frame is received by the transmitter). The last parameter in the data set element is l which represents the labeling. Labels “1” and “0” represent saturated and unsaturated Wi-Fi networks respectively. Based on this approach, 20,000 sample elements are collected with a more or less equal portion of saturated and unsaturated traffic scenarios. With this dataset size, few sample elements of a specific network configuration are used for training. However, we have observed that increasing the dataset beyond 20,000 does not produce significant improvement on the performance of the model. This shows that the granularity of the parameter setting in our training is small enough to achieve good accuracy even though few sample elements are

considered for each certain situation. From our inspection on different parameter configurations, we have observed that the IFS distribution does not change significantly for fixed packet size, traffic load, and CW_{min} (if the number of active nodes does not change significantly) and this leads to higher accuracy even if few sample elements are considered for each network configuration.

B. CNN STRUCTURE

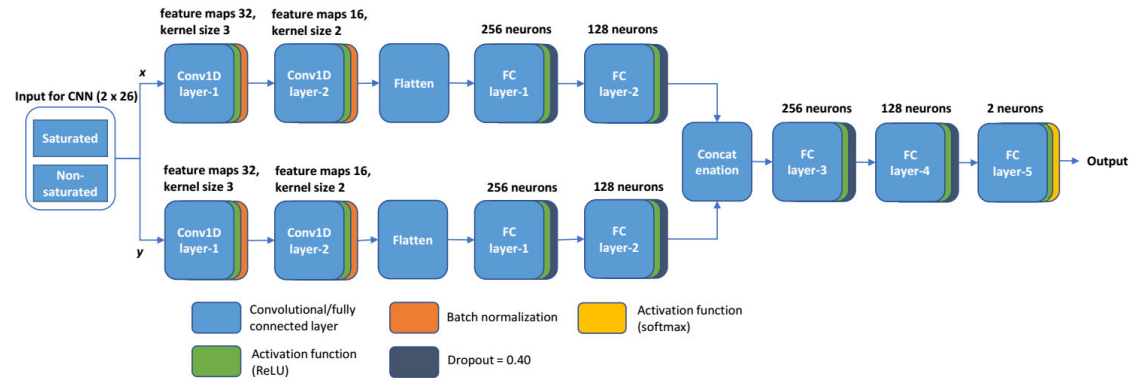
Since we have different types of features (i) histogram of IFS (26 values of x and 26 values of y), (ii) average IFS duration (σ - single value), and (iii) percentage of frame collision (ρ - single value), three CNN architectures were designed (Figure 5) each one using different combinations of the three features. Figure 5(a) shows a CNN architecture with two horizontal branches and each branch is associated with 26 values of x and y . Further, each branch comprises two 1D convolutional layers and two fully connected layers. The two 1D convolutional layers use feature maps and kernel size of: Conv1D layer-1 (feature maps 32, kernel size 3) and Conv1D layer-2 (feature maps 16, kernel size 2). Both the branches are concatenated at the concatenation point and after that three more fully connected layers are used. The hyperparameters including feature maps, kernel size, number of layers, neurons count, etc., are selected because they give best accuracy and generalization performance. The last fully connected layer of the architecture is the softmax layer and comprises 2 neurons. The output of 2 neurons represents the two classes: ‘saturated traffic’ and ‘unsaturated traffic’. This CNN architecture only relies on the histogram of IFS.

Figure 5(b) shows a CNN architecture that is based on two sets of features (i) histogram of IFS (26 values of x and 26 values of y) and (ii) average IFS duration (σ - single value). The two input features correspond to three branches in the CNN architecture where the first two branches correspond to the histogram of IFS and the third branch corresponds to the average IFS duration.

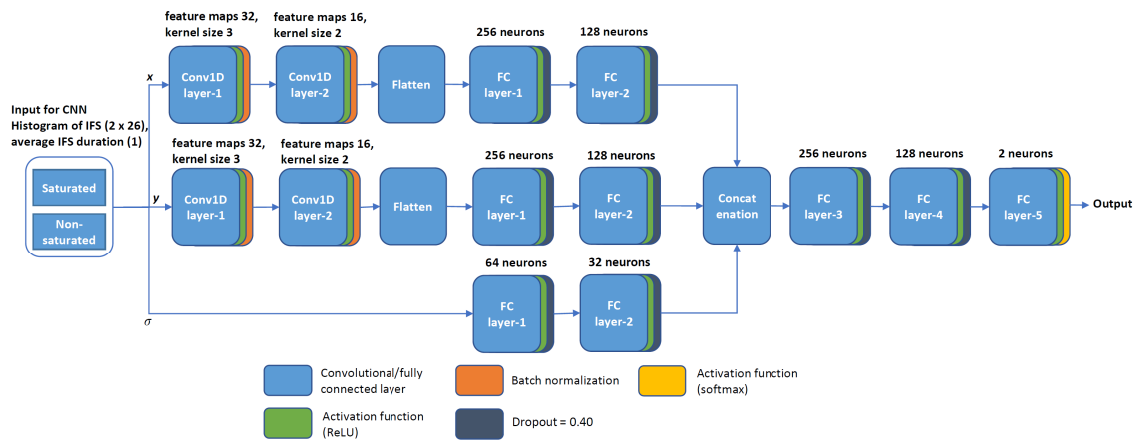
Similarly, Figure 5(c) shows a CNN architecture that is based on three sets of features (i) histogram of IFS (26 values of x and y), (ii) average duration of IFS (σ - single value), and (iii) percentage of frame collision (ρ - single value). The three input features correspond to four branches in the CNN architecture. The first two branches correspond to the histogram of IFS, the second branch corresponds to the average IFS duration, and the third branch corresponds to the percentage of frame collision.

The goal of having three models with distinct input features is to analyze which input feature combinations are more relevant in the classification of saturated and unsaturated Wi-Fi networks.

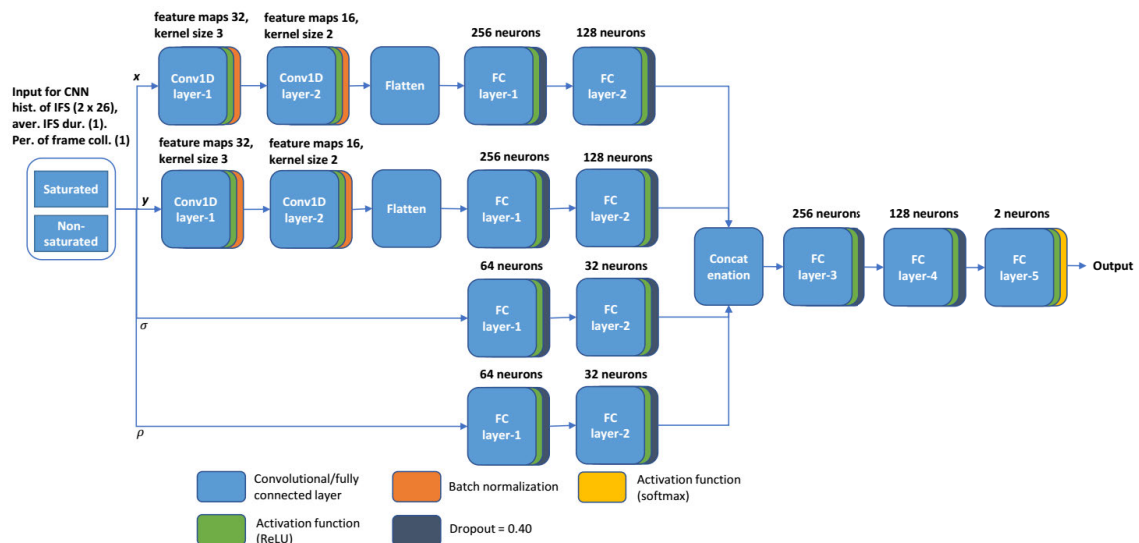
We captured two datasets: (i) training and validation and (ii) test. The total number of sample elements in the training and validation dataset are 20,000, as mentioned earlier. Each sample element has a size of (1 x 54) elements and it is further divided into three features: (1 x 52) or two times 26 values of the histogram of IFS, (1 x 1) single value



(a)



(b)



(c)

FIGURE 5. Convolutional Neural Network Architecture for a) model based on the histogram data of IFS b) model based on histogram data of IFS and average IFS duration c) model based on histogram data of IFS, average IFS duration, and percentage of frame collision.

of the average IFS duration, and (1 x 1) single value of the percentage of frame collision. For training of the three classifiers, we divided the data into training and validation datasets with a split of 70/30 and the whole dataset was normalized using *StandardScaler* from sklearn python. For the optimizer, the Adam optimizer [50] was used as it gave the best accuracy performance. In addition, *ReduceLROnPlateau* was used from Tensorflow because it helped in reducing the learning rate from 0.001 to 0.0001 when the validation loss stopped improving. In order to have a good balance between overfitting and underfitting, a batch size of 512 and a dropout of 0.40 were used. The total number of sample elements in the test dataset are 500 and this test set was captured intentionally in the grey region of the dataset used and in a Wi-Fi network configuration where hidden terminal problem occurs. The concern of generating the test dataset in the grey region and hidden node problem cases is to check the accuracy of the three models i.e., how well they identify such corner case sample elements. The training and test datasets are publicly available and can be used by other researchers.¹

C. IMPLEMENTATION PLATFORM

The neural network algorithm framework is developed based on Python 3.9.0 with Tensorflow 1.1.0 and Keras 2.2.5. Keras is a high-level application programming interface for neural networks written in Python and it is designed to run seamlessly on top of both Central Processing Unit and Graphics Processing Unit. Different Wi-Fi network scenarios were modeled using ns-3.31 to generate the training/testing datasets which are used to train and validate the proposed CNN models. In our setup, we have used a NVIDIA GTX 1080 Ti GPU that incorporates 3584 NVIDIA Cuda cores.

Here we discuss the scalability and time complexity of the proposed saturation classification solution. In this work, a wide range of Wi-Fi network scenarios are investigated. Wi-Fi networks that have 1-50 active nodes with a traffic load which varies in a wide range from a very low traffic load to high traffic load (beyond the capacity of the network) are considered in this work and the range of scenarios considered in the study cover most practical Wi-Fi network deployments. This work considers a clean channel environment where noise and interference from other networks are not considered. However, our saturation classification models solely depend on statistics of spacing duration between consecutive Wi-Fi frames (IFS and average IFS duration) coming from an efficient technology recognition system. Our previous works on technology recognition for identifying LTE and Wi-Fi technologies operate accurately in different complex environments in the presence of multiple access points and stations [16]. This confirms that the proposed saturation classification solution can also operate in different complex environments with varying access points and stations. In most practical applications, the traffic load of

Wi-Fi networks doesn't change significantly at least for few seconds [51].

The first step in the proposed saturation sensing scheme is capturing the I/Q samples of the wireless signal from the medium and classifying Wi-Fi frames. To estimate the Wi-Fi traffic load we generate an IFS histogram based on IFS values of Wi-Fi frames captured in a period of 1s. In our simulation, we use a discrete event simulator (ns-3) and parameter parsing is done by functions and hence the collection of Wi-Fi frame statistics occurs incurring negligible processing latency. However, in real time implementations, a technology recognition solution is required to capture, pre-process and classify the Wi-Fi frames on the medium. In our model the LTE eNB captures I/Q samples to classify Wi-Fi frames and there is no need for Wi-Fi packet decoding. In our previous work [52], we have seen that the capturing I/Q samples, pre-processing and classifying process requires a total of 951ms (average over 100 runs, using NVIDIA Jetson Nano for executing a wireless technology recognition system) for wireless signals measured in 1 second. Once the wireless technologies are classified from the measured wireless signal, the Wi-Fi frames are used to generate an IFS histogram which is used by the trained model to classify the saturation status of the Wi-Fi network. Executing this process takes an average processing time of 81ms (average over 100 runs). Therefore, in practical systems the proposed system requires an end-to-end processing time of 1.032s. In the proposed Wi-Fi saturation sensing scheme, the model is proposed to report the saturation status every T seconds. The period T can be optimally selected based on the traffic dynamics of the co-located networks. For a very dynamic traffic the value of T has to be set low. On the other hand, this value can be increased for less dynamic traffic to reduce computational overhead. However, this optimal selection of period T is not in the scope of this work. Generally, it can be observed that the processing time of the proposed scheme will have a negligible impact on implementing real-time coexistence decisions.

One of the challenges of implementing such ML based models is that the training of the ML model requires GPU hardware. In practical implementations, the model can be trained on GPUs first and executed on CPUs (e.g. the proposed model can be executed on the CPU of LTE eNB to enhance LTE and Wi-Fi coexistence). There is also a recent trend in ML which involves executing ML models on embedded platforms e.g., NVIDIA Jetson Nano, microcontrollers, etc by using model quantization. For instance, our recent work uses a NVIDIA Jetson Nano for executing a CNN model for recognition of wireless technologies [52]. However, the focus in this work is not on model quantization and we leave this out for future investigations. Hence, it has been validated that the model can be trained offline on a more powerful GPU and implemented on commodity CPU devices for real-time operation by the coexisting technologies.

Despite the need for GPU based training, the implementation of the proposed solution is less complex than traditional approaches which consider deployment of a central

¹<https://gitlab.ilabt.imec.be/mgirmay/ML-enabled-wi-fi-saturation-sensing>

coordinator and they require huge information exchange overhead for exchanging information with the co-located networks through a collaboration protocol. Whereas the proposed ML approach does not require such information exchange with the co-located network and the information about Wi-Fi saturation can be acquired on the eNB side by executing the ML model. In general, our model is proposed to be implemented in wireless technologies co-located with Wi-Fi and there are no any modifications required in the Wi-Fi side. Hence, our solution has no effect on implementation complexity of the Wi-Fi networks and this goes in line with Wi-Fi own goals of simple implementation.

VI. PERFORMANCE EVALUATION

A. MODEL PERFORMANCE

In the previous section, we have described 3 different CNN models that can be used to classify saturated and unsaturated Wi-Fi networks. The models are trained by splitting the dataset into training and testing datasets with a split of 70/30. Table 4 shows the performance of the three proposed CNN models in terms of different metrics including accuracy on validation dataset, accuracy on corner case test dataset, and model parameters. In the table, *Model a* represents the CNN model based on IFS histogram only whereas *Model b* refers to the CNN based on IFS histogram and average IFS duration. Similarly, *Model c* refers to the CNN model based on IFS histogram, IFS duration and Collision percentage. Initially, the accuracy of the models is evaluated by testing the performance of the CNN models on the validation dataset. In terms of accuracy on the validation dataset, the results show that the CNN model based on the histogram of IFS only outperforms the other two models.

TABLE 4. Performance of CNN models proposed to classify saturated and unsaturated Wi-Fi network.

Model Type	Accuracy on validation dataset	Accuracy on corner case test set	Model parameters
<i>Model a</i>	98.01%	94.8%	356,258
<i>Model b</i>	97.42%	94.3%	366,660
<i>Model c</i>	97.56%	94.1%	377,062

The performance of the models is also evaluated on a special test dataset which is obtained based on corner case scenarios. This performance evaluation is done to validate if the CNN models can accurately classify saturated and unsaturated Wi-Fi networks in corner case scenarios. The test set considered in this evaluation includes traffic scenarios which lie in the grey region of the training dataset. This special test set also includes Wi-Fi network configurations with hidden node problems. The results show that the IFS histogram based CNN model performs better than the other proposed models. In the corner case dataset, the IFS histogram based CNN model can classify saturated and unsaturated Wi-Fi networks at an accuracy of 94.8% (Table 4).

Based on the performance evaluation on the validation and test datasets, we can observe that the CNN model based on IFS histogram performs better than the other proposed

CNN models. This CNN model also has simpler CNN layer architecture (Figure 5) and fewer model parameters (Table 4) which make it a better option for practical implementations. The IFS histogram based model outperforms the other models as the features of the IFS histogram indirectly reflect the average IFS value and collision percentage. The IFS duration between a successfully decoded frame and its corresponding ACK frame is $16 \mu s$ (which is the SIFS). Hence, the frequency count of this SIFS value in the IFS histogram indicates the number of ACK frames, which indirectly reflects the percentage of collisions. Furthermore, if few active nodes (e.g. 1 or 2 active nodes) are considered, the collision percentage remains low even if the traffic load is high enough to exceed the saturation point and this can mislead the classification of saturated and unsaturated Wi-Fi networks.

B. CONFUSION MATRIX

In order to further investigate the performance of the proposed CNN models on classifying saturated and unsaturated Wi-Fi networks, we visualized the confusion matrix of the CNN models for the validation datasets, as presented in Figure 6 for the three CNN models. In this figure, each column stands for the true label (saturated and unsaturated Wi-Fi networks) and each row represents for the predicted labels. The CNN-predicted tags and the true labels indicate a high accuracy for all proposed CNN models.

C. ACCURACY AND LOSS CURVES

After analyzing the performance of the proposed CNN models, we have observed that the IFS histogram based CNN model is the best in terms of accuracy and simplicity. In this section, the accuracy and loss curves of this model are presented. The accuracy and loss curves are obtained in a complete CNN training process by testing the performance of the model on the 30% of the total dataset samples which are used to validate the CNN model. Figure 7(b) and Figure 7(a) show the accuracy and loss curves of the CNN model respectively. The results show that the model has a fast convergence on both classification accuracy and loss.

D. SYSTEM ILLUSTRATION

Figure 8 shows IFS histogram of saturated and unsaturated Wi-Fi networks in the grey region of the dataset used to train the CNN models. The Figure shows the values of $\{x_1, x_2, \dots, x_{26}, y_1, y_2, \dots, y_{26}\}$ which are generated based on the procedure described in Section V-A. The histograms presented in this graph are obtained by configuring 10 active nodes that use CW_{min} of 15 and CW_{max} is set to 1023. For this specific configuration, the cumulative PAR of saturation point (PAR_{sat}) is determined to be 2260 packets/s, i.e. 226 packets/s for each active node. The IFS histograms for unsaturated and saturated Wi-Fi networks shown in Figure 8 are generated by setting the cumulative PAR of the 10 active nodes to 2200 packet/s and 2300 packet/s respectively. From the classification decision outcome of the trained model, it can be observed that our IFS histogram based CNN model

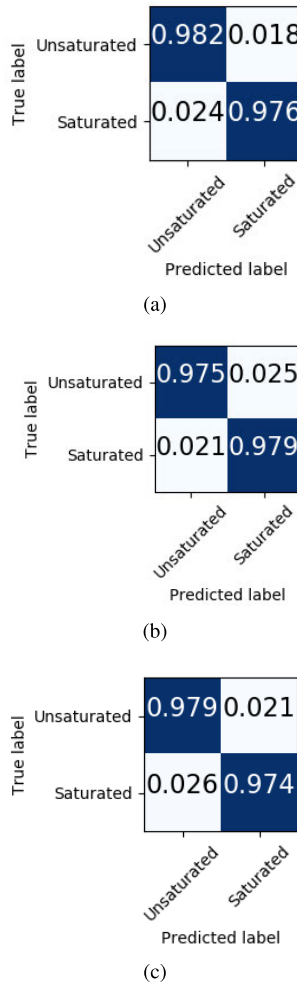


FIGURE 6. Confusion matrix a) CNN based on IFS histogram b) CNN based on IFS histogram and average IFS c) CNN based on IFS histogram, average IFS and collision percentage.

can accurately classify them despite a very similar distribution pattern.

E. COMPARISON OF THE PROPOSED SCHEME WITH EXISTING WI-FI LOAD ESTIMATION TECHNIQUES

In Section II we have reviewed many coexistence schemes and approaches used to estimate the load of a Wi-Fi network. Most of the existing coexistence studies assume that there is a signaling protocol which is available between co-located networks to inform the networks about the current load, or they can decode Wi-Fi traffic. However, there are also some techniques proposed to estimate the load in a Wi-Fi network. Mostly, Estimation of Number of Active Nodes (ENAN) [29]–[31], or computation of COT [16], [34] are used to estimate the traffic load of Wi-Fi network. Table 5 shows the load estimation reports of the ENAN based, COT based and the proposed Wi-Fi load estimations in different scenarios. The network configurations used for this performance comparison are *Config-1* (AN = 2, PAR = 1000 packets/s/AN, packet size = 1500 bytes), *Config-2* (AN = 2, PAR = 2000 packets/s/AN, packet size = 500 bytes), *Config-3* (AN = 20, PAR = 100 packets/s/AN,

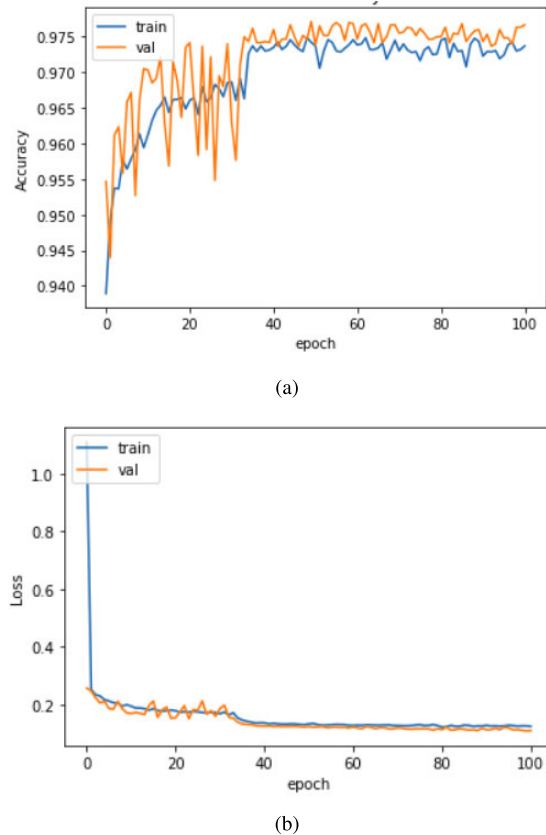


FIGURE 7. Performance of CNN based on IFS histogram a) model accuracy b) model loss.

TABLE 5. Wi-Fi traffic load estimation outcomes based on different approaches.

Configuration	Load estimation based on		
	ENAN	COT%	Proposed model
<i>Config-1</i>	low load	51.4	unsaturated
<i>Config-2</i>	low load	60.7	saturated
<i>Config-3</i>	high load	66.8	unsaturated
<i>Config-4</i>	high load	71.5	saturated

packet size = 1500 bytes), and *Config-4* (AN = 20, PAR = 150 packets/s/AN, packet size = 500 bytes).

As it can be observed from the configurations used, 2 and 20 active nodes with packet sizes of 500 byte and 1500 byte are considered for the performance comparison. The CW_{min} was configured to 15 and CW_{max} was set 1023. ENAN based load estimation uses the number of active nodes to estimate the Wi-Fi and gives wrong load estimations in *Config-2* (few AN with high PAR each) and *Config-3* (many AN with low PAR each). We can also observe that *Config-2* is saturated and has a COT of 60.7% on contrary *Config-3* is unsaturated with a COT of 66.8%. Hence, it is not easy to distinguish saturated and unsaturated Wi-Fi networks using COT. On the other hand, Table 5 shows that the proposed solution can accurately classify the saturated and unsaturated Wi-Fi traffic loads. In general, it can be observed that the proposed model outperforms the existing schemes as it does not require any

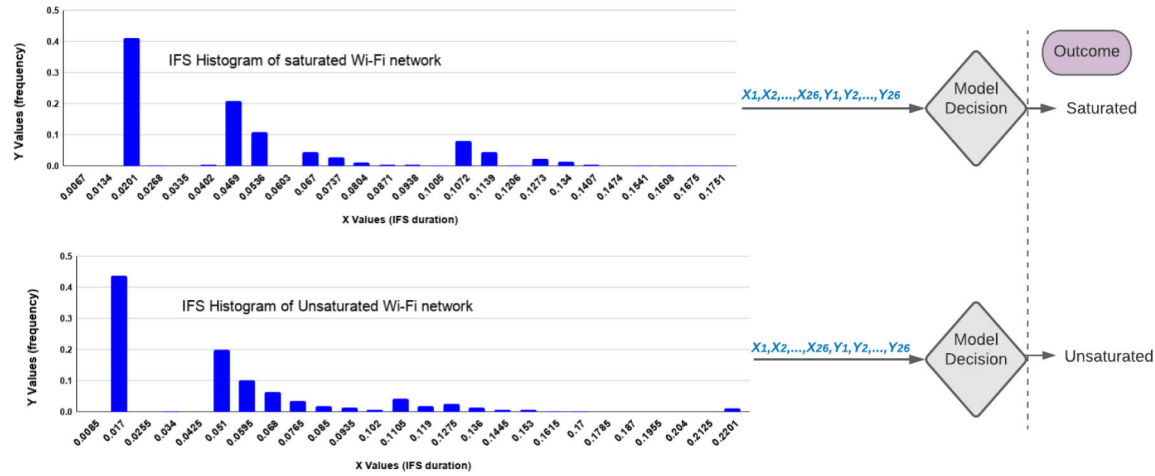


FIGURE 8. Test examples on histogram of interframe spacing for saturated and unsaturated Wi-Fi networks in the grey region and respective decision outcomes of the CNN model.

signaling protocol and is capable to distinguish between saturated and unsaturated Wi-Fi networks accurately.

F. MODEL GENERALITY

Initially, we generated our training dataset based on IEEE802.11a standard. We used this standard as a basic Wi-Fi standard with basic Distributed Coordination Function (DCF) without frame aggregation was preferred for automated collection of dataset that covers a wide range of saturated and unsaturated network scenarios using ns-3 simulator. Over the last years, recent IEEE802.11 standards have included several enhancements to the MAC and PHY layers including frame aggregation, multi-channel operation, MIMO and more. However, our CNN model uses the statistics of IFS to determine Wi-Fi saturation. The IFS statistics depend on the contention based MAC protocol, which is used by the recent IEEE 802.11 standards too. Table 7 is presented to illustrate this. The table shows the frame count and percentage of contention window sizes selected in 5000 sample frames taken from IEEE802.11a and IEEE802.11n saturated Wi-Fi networks. A saturated IEEE802.11a network which has 8 active nodes with PAR of 400 packets/sec/AN is used to generate the contention window count distribution shown in the table. Similarly, 8 active nodes which use PAR of 1000 packets/sec/AN are used to observe the contention window update of saturated IEEE802.11n network. Packet size of 1500bytes, CW_{min} of 15 and CW_{max} of 1023 are used for both networks (the rest parameters are similar to the ones in Table 1 for IEEE802.11a and Table 6 for IEEE802.11n).

The IEEE802.11n network is saturated at higher load due to its frame aggregation feature which boosts its capacity (Figure 9). The saturation throughput values for each IEEE802.11 standard were obtained by using 1, 10, 20, 30, 40, and 50 active nodes. Packet size of 1500bytes, CW_{min} of 15 and CW_{max} of 1023 are used for both networks.

TABLE 6. Parameters used to model saturated and unsaturated IEEE802.11n networks.

Parameter	Value
Bandwidth (MHz)	20
Carrier frequency (MHz)	5180
Packet size (bytes)	1500
Traffic model	UDP
CW _{min}	15
CW _{max}	1023
Slot duration (μ s)	9
Number of ANs	1-8
SIFS (μ s)	16
DIFS (μ s)	34
Frame aggregation	Yes
MIMO	No
PAR (packets/sec)	100-8000

The rest simulation parameters are set based on Table 1 and Table 6 for IEEE802.11a and IEEE802.11n networks respectively. Furthermore, the duration of aggregated frames in the IEEE802.11n network is much longer than the duration of single frames transmitted in IEEE802.11a network. The IFS values depend on the slot time, SIFS, DIFS, backoff time, and idle time. The slot time, SIFS, and DIFS are 9 μ s, 16 μ s, and 34 μ s for the Wi-Fi standards in 5 GHZ (IEEE 802.11a, IEEE 802.11n, IEEE 802.11ac). The backoff time is selected based on the contention window update selected in each transmission which depends on the number of active nodes that simultaneously contend to access the medium, or in other words, on the number of collisions, that is valid in all the IEEE802.11 standards. The CW_{min} and CW_{max} used in the 5 GHz Wi-Fi standards are 15 and 1023 respectively and this makes the range of backoff time used in each transmission/retransmission similar in the standards. Therefore, we can observe that frame aggregation feature introduced in the recent Wi-Fi standards does not affect our CNN model which uses IFS statistics to classify saturated and unsaturated Wi-Fi networks.

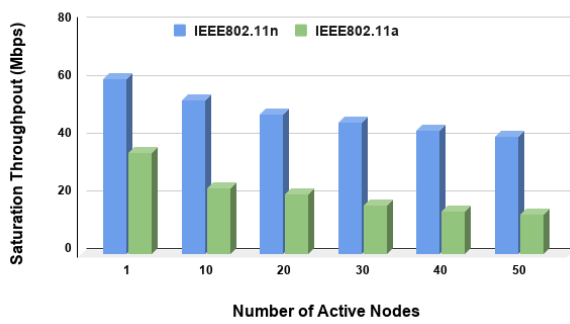


FIGURE 9. Saturation throughput of IEEE802.11a and IEEE802.11n for CW_{min} of 15 and CW_{max} of 1023.

TABLE 7. Contention window distribution for IEEE802.11a and IEEE802.11n saturated networks.

CW Size	IEEE802.11a CW Count	IEEE802.11a %	IEEE802.11n CW Count	IEEE802.11n %
15	2197	43.94	2166	43.32
31	2085	41.7	2091	41.82
63	465	9.3	471	9.42
127	171	3.42	168	3.36
255	52	1.04	59	1.18
511	21	0.42	31	0.62
1023	9	0.18	14	0.28

We can observe that the contention window percentage distributions of saturated Wi-Fi networks have similar trend in both IEEE802.11 standards (Table 7). This indicates that the IFS histogram of saturated Wi-Fi networks have similar distribution trends even if we consider different IEEE802.11 standards (in 5 GHz). Hence, our CNN model trained based on a dataset generated using IEEE802.11a is generic, and can be used to determine the Wi-Fi saturation of other IEEE802.11 standards as well. This is validated using a test set generated by modelling saturated and unsaturated IEEE802.11n networks. This test set was generated based on the dataset preparation described in Section V-A by fairly representing saturated and unsaturated IEEE802.11n networks. The test set was generated by varying the active nodes between 1 and 8 while PAR was varied between 100 packet/s and 8000 packet/s. Packet size of 1500bytes, CW_{min} of 15 and CW_{max} of 1023 are used for the test set collection (Table 6). This test set is also made available along with the training dataset. Using this test set, the developed CNN model that was trained by the dataset generated using IEEE802.11a networks can distinguish saturated and unsaturated IEEE802.11n networks at an accuracy of 96%. All in all, there is a strong indication that the CNN model can be used to sense saturation of Wi-Fi networks for different Wi-Fi evolutions, as long as the basic DCF operation mode is used.

Similar to most of the existing coexistence solution schemes, a Wi-Fi network with 20 MHz bandwidth is used to generate our training dataset. In our system model discussion we have described that our CNN model uses the IFS histogram which is generated from Wi-Fi frame statistics obtained by a technology recognition proposed in our

previous work in [16] which is trained and validated for 20 MHz Wi-Fi networks. For this reason, we used 20 MHz bandwidth to train and validate our Wi-Fi saturation sensing model. As Wi-Fi deployments on 40 MHz and 80 MHz are increasing recently [53], the technology recognition and Wi-Fi saturation sensing models can be trained and validated by generating datasets at different Wi-Fi bandwidths (e.g. 40 MHz, 80 MHz) using similar procedures used in our implementation for the 20 MHz bandwidth.

VII. CONCLUSION AND FUTURE WORK

In this work, three CNN based Wi-Fi network saturation sensing schemes are proposed for classifying saturated and unsaturated Wi-Fi networks avoiding the need for exchanging signaling messages between the co-located technologies and/or the need for decoding Wi-Fi frames. The CNN models used to determine the saturation status of Wi-Fi network are based on medium occupation statistics collected from the Wi-Fi frames. ns-3 simulator is used to model the Wi-Fi network used to generate a huge dataset with statistics information used in the CNN models. The first CNN model is developed based on IFS histogram of transmitted Wi-Fi frames, whereas the second model uses this histogram of IFS and the average IFS duration. The third proposed CNN model is developed based on the histogram of IFS, average IFS duration and percentage of frame collision observed on the medium. Simulation results demonstrate that all proposed models can accurately classify saturated and unsaturated Wi-Fi networks. Among the three proposed models, we have observed that the CNN model based on the IFS histogram only has the best accuracy performance and less complexity.

In the near future, this work will be validated by implementing the proposed Wi-Fi network saturation classification models in an experimental setup based on COTS devices where the frame statistics will be obtained in real-time. Furthermore, this work can be extended by implementing and analyzing a coexistence scheme that uses our Wi-Fi network saturation sensing model as input to select the right coexistence parameters. For example, optimal TxOP values of LTE LAA system can be selected based on the output of the Wi-Fi network saturation classification scheme proposed in this work. The optimal TxOP selection can be made more robust by implementing a Q-learning based solution, where the states used in the state/action table of the learning procedure are derived based on the outcomes of the saturation sensing approach proposed in this work.

REFERENCES

- [1] VNI CISCO. (2018). *CISCO Visual Networking Index: Forecast and Trends 2017–2022*. [Online]. Available: <https://davidellis.ca/wp-content/uploads/2019/05/cisco-vni-feb2019.pdf>
- [2] K. Lueth. (Jan. 2020). *Iot 2019 in Review: The 10 Most Relevant IoT Developments of the Year*. [Online]. Available: <https://iot-analytics.com/iot-2019-in-review/>
- [3] G. Naik, J. Liu, and J.-M. Park, “Coexistence of wireless technologies in the 5 GHz bands: A survey of existing solutions and a roadmap for future research,” *IEEE Commun. Surveys Tuts.*, vol. 20, no. 3, pp. 1777–1798, 3rd Quart., 2018, doi: [10.1109/COMST.2018.2815585](https://doi.org/10.1109/COMST.2018.2815585).

- [4] B. Chen, J. Chen, Y. Gao, and J. Zhang, "Coexistence of LTE-LAA and Wi-Fi on 5 GHz with corresponding deployment scenarios: A survey," *IEEE Commun. Surveys Tuts.*, vol. 19, no. 1, pp. 7–32, 1st Quart., 2017, doi: [10.1109/COMST.2016.2593666](https://doi.org/10.1109/COMST.2016.2593666).
- [5] FCC News Releas. (2020). *FCC Adopts New Rules for the 6 GHz Band, Unleashing 1, 200 Megahertz of Spectrum for Unlicensed Use*. [Online]. Available: <https://docs.fcc.gov/public/attachments/DOC-363945A1.pdf>
- [6] S. Manzoor, Y. Yin, Y. Gao, X. Hei, and W. Cheng, "A systematic study of IEEE 802.11 DCF network optimization from theory to testbed," *IEEE Access*, vol. 8, pp. 154114–154132, 2020, doi: [10.1109/ACCESS.2020.3018088](https://doi.org/10.1109/ACCESS.2020.3018088).
- [7] *Evolved Universal Terrestrial Radio Access (E-UTRA); Physical Layer Procedures*, document TS 36.213 V13.3.0. Release 13, 3GPP, New Orleans, LA, USA, 2016.
- [8] *The Prospect LTE Wi-Fi Sharing Unlicensed Spectrum*, Qualcomm, San Diego, CA, USA, Feb. 2015. [Online]. Available: <https://www.qualcomm.com/documents/prospect-lte-and-wi-fi-sharing-unlicensed-spectrum-srg-whitepaper>
- [9] Qualcomm. (Jul. 2017). *Private LTE Networks*. [Online]. Available: <https://www.qualcomm.com/media/documents/files/private-lte-networks.pdf>
- [10] R. Bajracharya, R. Shrestha, and H. Jung, "Future is unlicensed: Private 5G unlicensed network for connecting industries of future," *Sensors*, vol. 20, no. 10, p. 2774, May 2020, doi: [10.3390/s20102774](https://doi.org/10.3390/s20102774).
- [11] D. Jiang and L. Delgrossi, "IEEE 802.11p: Towards an international standard for wireless access in vehicular environments," in *Proc. IEEE Veh. Technol. Conf.*, Singapore, May 2008, pp. 2036–2040, doi: [10.1109/VETEC.2008.458](https://doi.org/10.1109/VETEC.2008.458).
- [12] R. Molina-Masegosa and J. Gozalvez, "LTE-V for sidelink 5G V2X vehicular communications: A new 5G technology for short-range vehicle-to-everything communications," *IEEE Veh. Technol. Mag.*, vol. 12, no. 4, pp. 30–39, Dec. 2017, doi: [10.1109/MVT.2017.2752798](https://doi.org/10.1109/MVT.2017.2752798).
- [13] V. Maglogiannis, D. Naudts, P. Willemen, and I. Moerman, "Impact of LTE operating in unlicensed spectrum on Wi-Fi using real equipment," in *Proc. IEEE Global Commun. Conf.*, Washington, DC, USA, Dec. 2016, pp. 1–6, doi: [10.1109/GLOCOM.2016.7841884](https://doi.org/10.1109/GLOCOM.2016.7841884).
- [14] Qualcomm Technologies. (Jul. 2017). *Qualcomm Research LTE in Unlicensed Spectrum: Harmonious Coexistence with Wi-Fi*. [Online]. Available: <https://www.qualcomm.com/media/documents/files/lte-unlicensed-coexistence-whitepaper.pdf>
- [15] G. Bianchi, "IEEE 802.11-saturation throughput analysis," *IEEE Commun. Lett.*, vol. 2, no. 12, pp. 318–320, Dec. 1998, doi: [10.1109/4234.736171](https://doi.org/10.1109/4234.736171).
- [16] V. Maglogiannis, A. Shahid, D. Naudts, E. De Poorter, and I. Moerman, "Enhancing the coexistence of LTE and Wi-Fi in unlicensed spectrum through convolutional neural networks," *IEEE Access*, vol. 7, pp. 28464–28477, 2019, doi: [10.1109/ACCESS.2019.2902035](https://doi.org/10.1109/ACCESS.2019.2902035).
- [17] F. Hao, C. Yongyu, H. Li, J. Zhang, and W. Quan, "Contention window size adaptation algorithm for LAA-LTE in unlicensed band," in *Proc. Int. Symp. Wireless Commun. Syst. (ISWCS)*, Poznan, Poland, Sep. 2016, pp. 476–480, doi: [10.1109/ISWCS.2016.7600951](https://doi.org/10.1109/ISWCS.2016.7600951).
- [18] S. Liu, R. Yin, and G. Yu, "Hybrid adaptive channel access for LTE-U systems," *IEEE Trans. Veh. Technol.*, vol. 68, no. 10, pp. 9820–9832, Oct. 2019, doi: [10.1109/TVT.2019.2933586](https://doi.org/10.1109/TVT.2019.2933586).
- [19] R. Yin, G. Yu, A. Maaref, and G. Y. Li, "LBT-based adaptive channel access for LTE-U systems," *IEEE Trans. Wireless Commun.*, vol. 15, no. 10, pp. 6585–6597, Oct. 2016, doi: [10.1109/TWC.2016.2586467](https://doi.org/10.1109/TWC.2016.2586467).
- [20] S. Han, Y.-C. Liang, Q. Chen, and B.-H. Soong, "Licensed-assisted access for LTE in unlicensed spectrum: A MAC protocol design," in *Proc. IEEE Int. Conf. Commun. (ICC)*, Kuala Lumpur, Malaysia, May 2016, pp. 1–6, doi: [10.1109/ICC.2016.7511104](https://doi.org/10.1109/ICC.2016.7511104).
- [21] E. Almeida, A. M. Cavalcante, R. C. D. Paiva, F. S. Chaves, F. M. Abinader, R. D. Vieira, S. Choudhury, E. Tuomaala, and K. Doppler, "Enabling LTE/WiFi coexistence by LTE blank subframe allocation," in *Proc. IEEE Int. Conf. Commun. (ICC)*, Budapest, Hungary, Jun. 2013, pp. 5083–5088, doi: [10.1109/ICC.2013.6655388](https://doi.org/10.1109/ICC.2013.6655388).
- [22] V. Maglogiannis, D. Naudts, A. Shahid, and I. Moerman, "A Q-learning scheme for fair coexistence between LTE and Wi-Fi in unlicensed spectrum," *IEEE Access*, vol. 6, pp. 27278–27293, 2018, doi: [10.1109/ACCESS.2018.2829492](https://doi.org/10.1109/ACCESS.2018.2829492).
- [23] R. Bajracharya, R. Shrestha, and S. W. Kim, "Q-learning based fair and efficient coexistence of LTE in unlicensed band," *Sensors*, vol. 19, no. 13, p. 2875, Jun. 2019, doi: [10.3390/s19132875](https://doi.org/10.3390/s19132875).
- [24] J. Tan, S. Xiao, S. Han, and Y.-C. Liang, "A learning-based coexistence mechanism for LAA-LTE based HetNets," in *Proc. IEEE Int. Conf. Commun. (ICC)*, Kansas City, MO, USA, May 2018, pp. 1–6, doi: [10.1109/ICC.2018.8422826](https://doi.org/10.1109/ICC.2018.8422826).
- [25] N. Bitar, M. O. Al Kalaa, S. J. Seidman, and H. H. Refai, "On the coexistence of LTE-LAA in the unlicensed band: Modeling and performance analysis," *IEEE Access*, vol. 6, pp. 52668–52681, 2018, doi: [10.1109/ACCESS.2018.2870757](https://doi.org/10.1109/ACCESS.2018.2870757).
- [26] A. Shahid, V. Maglogiannis, I. Ahmed, K. S. Kim, E. De Poorter, and I. Moerman, "Energy-efficient resource allocation for ultra-dense licensed and unlicensed dual-access small cell networks," *IEEE Trans. Mobile Comput.*, vol. 20, no. 3, pp. 983–1000, Mar. 2021, doi: [10.1109/TMC.2019.2953845](https://doi.org/10.1109/TMC.2019.2953845).
- [27] J. M. de C. Neto, S. F. G. Neto, P. M. de Santana, and V. A. de Sousa, "Multi-cell LTE-U/Wi-Fi coexistence evaluation using a reinforcement learning framework," *Sensors*, vol. 20, no. 7, p. 1855, Mar. 2020, doi: [10.3390/s20071855](https://doi.org/10.3390/s20071855).
- [28] Y. Su, X. Du, L. Huang, Z. Gao, and M. Guizani, "LTE-U and Wi-Fi coexistence algorithm based on Q-learning in multi-channel," *IEEE Access*, vol. 6, pp. 13644–13652, 2018, doi: [10.1109/ACCESS.2018.2803258](https://doi.org/10.1109/ACCESS.2018.2803258).
- [29] V. Sathyia, M. Mehrnoush, M. Ghosh, and S. Roy, "Energy detection based sensing of multiple Wi-Fi BSSs for LTE-U CSAT," in *Proc. IEEE Global Commun. Conf.*, Abu Dhabi, United Arab Emirates, Dec. 2018, pp. 1–7, doi: [10.1109/GLOCOM.2018.8647217](https://doi.org/10.1109/GLOCOM.2018.8647217).
- [30] V. Sathyia, M. Mehrnoush, M. Ghosh, and S. Roy, "Auto-correlation based sensing of multiple Wi-Fi BSSs for LTE-U CSAT," in *Proc. IEEE 90th Veh. Technol. Conf. (VTC-Fall)*, Honolulu, HI, USA, Sep. 2019, pp. 1–7, doi: [10.1109/VTCFall.2019.8891109](https://doi.org/10.1109/VTCFall.2019.8891109).
- [31] A. Dziedzic, V. Sathyia, M. I. Rochman, M. Ghosh, and S. Krishnan, "Machine learning enabled spectrum sharing in dense LTE-U/Wi-Fi coexistence scenarios," *IEEE Open J. Veh. Tech.*, vol. 1, pp. 173–189, 2020, doi: [10.1109/OJVT.2020.2981519](https://doi.org/10.1109/OJVT.2020.2981519).
- [32] H. Gu, Y. Wang, S. Hong, and G. Gui, "Deep learning aided friendly coexistence of WiFi and LTE in unlicensed bands," in *Proc. 11th Int. Conf. Wireless Commun. Signal Process. (WCSP)*, Xi'an, China, Oct. 2019, pp. 1–5, doi: [10.1109/WCSP.2019.8928141](https://doi.org/10.1109/WCSP.2019.8928141).
- [33] J. Fontaine, E. Fonseca, A. Shahid, M. Kist, A. DaSilva, I. Moerman, and E. de Poorter, "Towards low-complexity wireless technology classification across multiple environments," *Ad Hoc Netw.*, vol. 91, pp. 1570–18705, 2019, doi: [10.1016/j.adhoc.2019.101881](https://doi.org/10.1016/j.adhoc.2019.101881).
- [34] M. Girmay, V. Maglogiannis, D. Naudts, J. Fontaine, A. Shahid, E. De Poorter, and I. Moerman, "Adaptive CNN-based private LTE solution for fair coexistence with Wi-Fi in unlicensed spectrum," in *Proc. IEEE Conf. Comput. Commun. Workshops*, Toronto, ON, Canada, Jul. 2020, pp. 346–351, doi: [10.1109/INFOCOMWKSHPS50562.2020.9162663](https://doi.org/10.1109/INFOCOMWKSHPS50562.2020.9162663).
- [35] P. Soto, M. Camelo, J. Fontaine, M. Girmay, A. Shahid, V. Maglogiannis, E. Poorter, I. Moerman, F. Botero, and S. Latrâ, "Augmented Wi-Fi: An AI-based Wi-Fi management framework for Wi-Fi/LTE coexistence," in *Proc. 16th Int. Conf. Netw. Service Manag. (CNSM)*, Izmir, Turkey, 2020, pp. 1–9, doi: [10.23919/CNSM50824.2020.9269064](https://doi.org/10.23919/CNSM50824.2020.9269064).
- [36] N. Rastegardoost and B. Jabbari, "A machine learning algorithm for unlicensed LTE and WiFi spectrum sharing," in *Proc. IEEE Int. Symp. Dyn. Spectr. Access Netw. (DySPAN)*, Seoul, South Korea, Oct. 2018, pp. 1–6, doi: [10.1109/DySPAN.2018.8610489](https://doi.org/10.1109/DySPAN.2018.8610489).
- [37] J. Tan, L. Zhang, Y.-C. Liang, and D. Niyato, "Deep reinforcement learning for the coexistence of LAA-LTE and WiFi systems," in *Proc. IEEE Int. Conf. Commun. (ICC)*, Shanghai, China, Dec. 2019, pp. 1–6, doi: [10.1109/ICC.2019.8761566](https://doi.org/10.1109/ICC.2019.8761566).
- [38] X. Lu, V. Petrov, D. Molchanov, S. Andreev, T. Mahmoodi, and M. Dohler, "5G-U: Conceptualizing integrated utilization of licensed and unlicensed spectrum for future IoT," *IEEE Commun. Mag.*, vol. 57, no. 7, pp. 92–98, Jul. 2019, doi: [10.1109/MCOM.2019.1800663](https://doi.org/10.1109/MCOM.2019.1800663).
- [39] P. Varga, J. Peto, A. Franko, D. Balla, D. Haja, F. Janky, G. Soos, D. Ficzere, M. Maliosz, and L. Toka, "5g support for industrial iot applications-challenges, solutions, and research gaps," *Sensors*, vol. 20, no. 3, p. 828, Feb. 2020, doi: [10.3390/s20030828](https://doi.org/10.3390/s20030828).
- [40] M. C. Lucas-Estañ, J. Gozalvez, and M. Sepulcre, "On the capacity of 5G NR grant-free scheduling with shared radio resources to support ultra-reliable and low-latency communications," *Sensors*, vol. 19, no. 16, p. 3575, Aug. 2019, doi: [10.3390/s19163575](https://doi.org/10.3390/s19163575).
- [41] I. Mistry, S. Tanwar, S. Tyagi, and N. Kumar, "Blockchain for 5G-enabled IoT for industrial automation: A systematic review, solutions, and challenges," *Mech. Syst. Signal Process.*, vol. 135, Jan. 2020, Art. no. 106382, doi: [10.1016/j.ymssp.2019.106382](https://doi.org/10.1016/j.ymssp.2019.106382).

- [42] N. Teslya and I. Ryabchikov, "Blockchain platforms overview for industrial IoT purposes," in *Proc. 22nd Conf. Open Innov. Assoc. (FRUCT)*, Jyvaskyla, Finland, May 2018, pp. 250–256, doi: [10.23919/FRUCT.2018.8468276](https://doi.org/10.23919/FRUCT.2018.8468276).
- [43] N. Patriciello, S. Lagen, B. Bojovic, and L. Giupponi, "NR-U and IEEE 802.11 technologies coexistence in unlicensed mmWave spectrum: Models and evaluation," *IEEE Access*, vol. 8, pp. 71254–71271, 2020, doi: [10.1109/ACCESS.2020.2987467](https://doi.org/10.1109/ACCESS.2020.2987467).
- [44] V. Sathy, S. M. Kala, M. I. Rochman, M. Ghosh, and S. Roy, "Standardization advances for cellular and Wi-Fi coexistence in the unlicensed 5 and 6 GHz bands," *GetMobile, Mobile Comput. Commun.*, vol. 24, no. 1, pp. 5–15, Aug. 2020, doi: [10.1145/3417084.3417086](https://doi.org/10.1145/3417084.3417086).
- [45] G. Naik, B. Choudhury, and J.-M. Park, "IEEE 802.11bd & 5G NR V2X: Evolution of radio access technologies for V2X communications," *IEEE Access*, vol. 7, pp. 70169–70184, 2019, doi: [10.1109/ACCESS.2019.2919489](https://doi.org/10.1109/ACCESS.2019.2919489).
- [46] G. Naik, J. Liu, and J.-M.-J. Park, "Coexistence of dedicated short range communications (DSRC) and Wi-Fi: Implications to Wi-Fi performance," in *Proc. IEEE Conf. Comput. Commun.*, Atlanta, GA, USA, May 2017, pp. 1–9, doi: [10.1109/INFOCOM.2017.8057214](https://doi.org/10.1109/INFOCOM.2017.8057214).
- [47] J. Liu, G. Naik, and J. J. Park, "Coexistence of DSRC and Wi-Fi: Impact on the performance of vehicular safety applications," *IEEE Int. Conf. Commun. (ICC)*, Paris, France, 2017, pp. 1–6, doi: [10.1109/ICC.2017.7996758](https://doi.org/10.1109/ICC.2017.7996758).
- [48] Y. Park and H. Kim, "On the coexistence of IEEE 802.11ac and WAVE in the 5.9 GHz band," *IEEE Commun. Mag.*, vol. 52, no. 6, pp. 162–168, Jun. 2014, doi: [10.1109/MCOM.2014.6829959](https://doi.org/10.1109/MCOM.2014.6829959).
- [49] *Propagation Loss Models NS-3*. Accessed: Jan. 10, 2021. [Online]. Available: <https://www.nsnam.org/docs/models/html/propagation.html>
- [50] D. Kingma and J. Ba, "Adam: A method for stochastic optimization," 2014, *arXiv:1412.6980*. [Online]. Available: <https://arxiv.org/abs/1412.6980>
- [51] R. Pries, F. Wamser, D. Staehle, K. Heck, and P. Tran-Gia, "On traffic characteristics of a broadband wireless Internet access," in *Proc. Next Gener. Internet Netw.*, Aveiro, Portugal, Jul. 2009, pp. 1–7, doi: [10.1109/NGI.2009.515772](https://doi.org/10.1109/NGI.2009.515772).
- [52] J. Fontaine, A. Shahid, R. Elsas, A. Seferagic, I. Moerman, and E. De Poorter, "Multi-band sub-GHz technology recognition on NVIDIA's Jetson Nano," in *Proc. IEEE Vehic. Tech. Conf.*, 2020, pp. 1–7. [Online]. Available: <http://hdl.handle.net/1854/LU-8683397>
- [53] V. Sathy, M. I. Rochman, and M. Ghosh, "Measurement-based coexistence studies of LAA & Wi-Fi deployments in Chicago," *IEEE Wireless Commun.*, vol. 28, no. 1, pp. 136–143, Feb. 2021, pp. 1–8, doi: [10.1109/WC.001.2000205](https://doi.org/10.1109/WC.001.2000205).



MERKEBU GIRMAY received the B.Sc. degree in electrical engineering and the M.Sc. degree in communication engineering from Mekelle University, Tigray, in 2010 and 2014, respectively. He is currently pursuing the Ph.D. degree with the Faculty of Engineering and Architecture, University of Ghent-imec, Belgium. After his studies, he worked as an Academic Staff with Mekelle University, where he was involved in national research projects and community service. In December 2018, he joined the IDLab, Department of Information Technology, University of Ghent-imec. He has experience in working on H2020 European Projects. His research interests include network planning and optimization, software defined radios, private networks, vehicular communications, 5G, LTE, and IEEE802.11.



ADNAN SHAHID (Senior Member, IEEE) received the B.Eng. and M.Eng. degrees in computer engineering from the University of Engineering and Technology, Taxila, Pakistan, in 2006 and 2010, respectively, and the Ph.D. degree in information and communication engineering from Sejong University, South Korea, in 2015. He is currently working as a Senior Researcher with IDLab, which is a core research group of imec with research activities embedded within Ghent University and the University of Antwerp. He is and has been involved in several ongoing and finished research projects: DARPA Spectrum Collaboration Challenge (SC2), European H2020 research projects, such as eWINE and WiSHFUL, European Space Agency FP7-CODYSUN, and national 42974.

projects, such as SAMURAI, IDEAL-IOT, and Cognitive Wireless Networking Management. He is the author or coauthor of more than 60 plus publications in well-known journals and conferences. His research interests include resource optimization, interference management, self-organizing networks, small cell networks, machine learning, artificial intelligence, and 5G and 6G networks. He is also serving as an Associate Editor for various journals, such as IEEE ACCESS and the *Journal of Networks and Computer Application (JNCA)*.



VASILIS MAGLOGIANNIS received the M.Eng. degree in computer engineering and the M.Sc. degree in science and technology of computers, telecommunications and networks from the University of Thessaly, Greece, in 2012 and 2014, respectively, and the Ph.D. degree in computer science engineering from the Department of Information Technology, Ghent University, in 2018. Since then, he has been working as a Postdoctoral Researcher with the IDLab, University of Ghent, in collaboration with imec, Belgium. His research interests include mobile and wireless networks, 5G and beyond, LTE, 802.11, cooperative intelligent transport systems (C-ITS), real-time software defined radio, and wireless sensor networks. He has experience in working on several bilateral/consultancy, national, and European research and development projects in collaboration with academic and industrial partners.



DRIES NAUDTS received the master's degree in computer science from Ghent University, Belgium, in 2001. After his studies, he started as a Software Engineer at Kresoft and Nisis. In April 2005, he joined the Intec Broadband Communication Networks Group, where he is currently working as a Senior Researcher. Since 2009, he has been with imec. He is also involved in research on broadband mobile and wireless communication. His research interests include advanced network architecture, mobile wireless networks, 4G, 5G, C-ITS, V2X, evolved packet core, IEEE 802.11, ad hoc and mesh networking, IPv6, and wireless testbed development. He is also working on several bilateral/consultancy, national, and European research and development projects in close collaboration with other academic and industrial partners.



INGRID MOERMAN (Member, IEEE) received the degree in electrical engineering and the Ph.D. degree from Ghent University, in 1987 and 1992, respectively. She became a part-time Professor at Ghent University in 2000. She is currently a Staff Member with IDLab, a core research group of imec with research activities embedded in Ghent University and the University of Antwerp. She is coordinating the research activities on mobile and wireless networking at Ghent University, where she is leading a research team of more than 30 members. She is also a Program Manager of the "Deterministic Networking" track at imec and in this role she coordinates research activities on end-to-end wired/wireless networking solutions driven by time-critical applications that have to meet strict QoS requirements in terms of throughput, latency bounds and dependability in smart application areas such as Industry 4.0, vehicular networks, and professional entertainment. Her research interests include cooperative and intelligent radio networks, real-time software defined radio, time-sensitive networks, dynamic spectrum sharing, coexistence across heterogeneous wireless networks, vehicular networks, open-source prototyping platforms, software tools for programmable networks, next generation wireless networks (5G/6G), and experimentally supported research. She has a longstanding experience in running and coordinating national and EU research funded projects. At the international level, she was leading team SCATTER, consisting of researchers from IMEC-IDLab and Rutgers University, USA, in the DARPA Spectrum Collaboration Challenge (SC2). The double prize winning SCATTER team was one of the ten finalists at the DARPA SC2 championship event organized at Mobile World Congress in LA (October 2019).

•••